Highly collimated monoenergetic target-surface electron acceleration in near-critical-density plasmas

J. Y. Mao, L. M. Chen, K. Huang, Y. Ma, J. R. Zhao, D. Z. Li, W. C. Yan, J. L. Ma, M. Aeschlimann, Z. Y. Wei, and J. Zhang

Citation: Applied Physics Letters **106**, 131105 (2015); doi: 10.1063/1.4916636
View online: http://dx.doi.org/10.1063/1.4916636
View Table of Contents: http://scitation.aip.org/content/aip/journal/apl/106/13?ver=pdfcov
Published by the AIP Publishing

Highly collimated monoenergetic target-surface electron acceleration in near-critical-density plasmas

J. Y. Mao,[1,2] L. M. Chen,[1,3,a)] K. Huang,[1] Y. Ma,[1] J. R. Zhao,[1] D. Z. Li,[1,4] W. C. Yan,[1] J. L. Ma,[1] M. Aeschlimann,[2] Z. Y. Wei,[1] and J. Zhang[5]
[1]*Beijing National Laboratory for Condensed Matter Physics, Institute of Physics, CAS, Beijing 100190, China*
[2]*Department of Physics and Research Center OPTIMAS, University of Kaiserslautern, Kaiserslautern 67663, Germany*
[3]*IFSA Collaborative Innovation Center, Shanghai Jiao Tong University, Shanghai 200240, China*
[4]*Institute of High Energy Physics, CAS, Beijing 100049, China*
[5]*Laboratory for Laser Plasmas (Ministry of Education) and Department of Physics and Astronomy, Shanghai Jiao Tong University, Shanghai 200240, China*

(Received 28 January 2015; accepted 20 March 2015; published online 1 April 2015)

Optimized-quality monoenergetic target surface electron beams at MeV level with low normalized emittance (0.03π mm mrad) and high charge (30 pC) per shot have been obtained from 3 TW laser-solid interactions at a grazing incidence. The 2-Dimension particle-in-cell simulations suggest that electrons are wake-field accelerated in a large-scale, near-critical-density preplasma. It reveals that a bubble-like structure as an accelerating cavity appears in the near-critical-density plasma region and travels along the target surface. A bunch of electrons are pinched transversely and accelerated longitudinally by the wake field in the bubble. The outstanding normalized emittance and monochromaticity of such highly collimated surface electron beams could make it an ideal beam for fast ignition or may serve as an injector in traditional accelerators. © *2015 AIP Publishing LLC*.
[http://dx.doi.org/10.1063/1.4916636]

The investigation of the fast electron jets generated in laser-plasma interactions, which have been observed in a number of works,[1–9] has remained a hot topic in the fast ignition[10,11] concept of the inertial confinement fusion (ICF). In these studies, the electron beams, emitted at an angle between laser specular and target normal direction, are caused by different well-established mechanisms, such as resonance absorption and vacuum heating. However, these electron beams suffer from large divergence angles and energy spectra that exhibit Maxwellian distributions.[12–15] Although several groups have demonstrated a peaked spectrum for out-going electron bunches,[16,17] disadvantages of these electron bunches (for instance, limited total charge and wide-band energy distribution) reduce the conversion efficiency from the driven laser energy to the electron energy deposited in the ignition center. The use of a reentrant cone target in ICF, which results in an enhancement in neutron yield by three orders of magnitude,[18,19] provides an idea for employing oblique incidence techniques in laser-solid interactions to study the fast electron jet along the target surface. The beam quality of the target surface electrons (TSEs) has been improved experimentally by increasing the laser incident angle, enhancing the laser intensity, and varying the preplasma scale length. The significance of the prepulse was emphasized[20] by optimizing the underdense preplasma environment for the TSE generation. All these previous results revealed the surface-electron behavior along the inner cone. The quality of the generated TSE is, however, still far from optimal (e.g., large beam divergence angle and large spread in energy). On the other hand, previous theoretical approaches[21–24] are only able to explain the mechanism that the preheated electrons are trapped by the strong self-generated electromagnetic field on the target surface and heated by the reflected laser field. However, these models cannot explain the extraordinarily small beam divergence angle and low energy spread of the highly collimated TSE beam. Therefore, a acceleration mechanism is required for clarifying the corresponding guiding and acceleration process during the laser-plasma interactions. Experimentally, in order to optimize the state-of-the-art TSE beam quality, the challenge is to produce an appropriate preplasma as an acceleration environment, such is crucial to produce highly collimated monoenergetic electron beams.

In this article, we present monoenergetic TSE beams with extraordinary low normalized emittance and large charge per shot from 3 TW laser-solid interactions at grazing incidence by optimizing the preplasma parameters in laser-Cu target interactions. This approach suggests a distinctive acceleration mechanism. A theoretical model is proposed to explain the experimentally observed TSE beam caused by the surface acceleration at about half MeV. 2-Dimensional (2D) particle-in-cell (PIC) simulations show that electrons are accelerated due to wake-field acceleration in the underdense preplasma.

The experiment was carried out by using a single-shot, 300 mJ Ti:sapphire laser working at a center wavelength of 800 nm. A schematic picture of the experimental layout is shown in Fig. 1. After reflected by two mirrors M_1 and M_2, the *p*–polarized laser pulse with duration $\tau_0 = 67$ fs was focused to a spot of 7 μm (FWHM) by a f/3.5 off-axis parabolic (OAP) mirror, which is incident onto a flat Cu target (Dia. 50 mm × 6 mm thick) at an angle of 72°. A prepulse with controlled intensity was applied 7 ns in advance of the

[a)]Author to whom correspondence should be addressed. Electronic mail: lmchen@iphy.ac.cn.

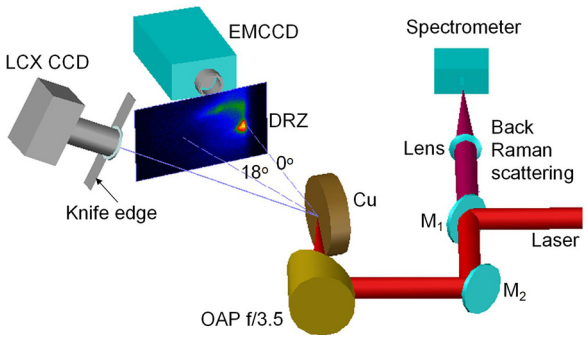

FIG. 1. Experimental setup. Dashed lines show the laser specular direction at 18° and target-surface direction at 0°.

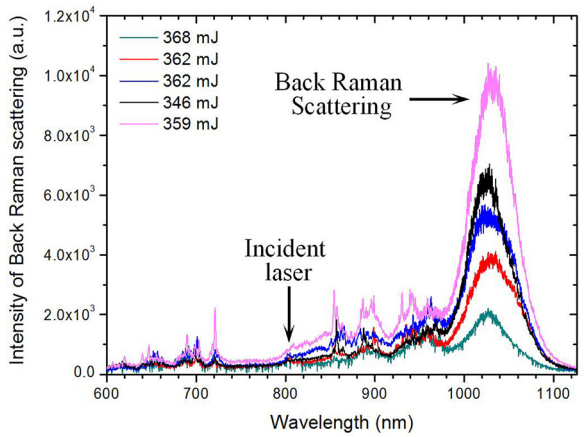

FIG. 2. Spectra for measuring the Back Raman Scattering during the laser solid interactions, where curves in different colors indicate various incident laser energies.

main pulse to produce the uniform underdense preplasmas. In order to detect the spatial angular distribution of the emitted electron beams, a DRZ (Diagonal Radioactive Zone) phosphor plate with a Andor EMCCD (Electron-multiplying Charge Coupled Device) was installed at a distance of approximately 150 mm from the laser focus spot. An electron spectrometer (ES) with a 0.1 T magnetic field was set along the target-surface direction, approximately within 5° from the target surface, to measure the energy spectrum of the TSE beams. The electrons from 5 keV to 2 MeV are recorded by an image plate (IP) (Fujifilm BAS-SR 2025).[25] Additionally, a spectrometer (Ocean Optics) is used to detect the preplasma density by measuring the stimulated back Raman scattering (SBRS) in single-shot mode.[26,27] Moreover, a single-photon-counting X-ray CCD (PI LCX CCD) combined with a knife edge is used for measuring the preplasma scale.[28]

First of all, we investigate quantitatively the characteristics of the generated preplasma, since an effective preplasma is crucial to produce the highly collimated TSE beam. To achieve an effective underdense preplasma, a prepulse with an adjustable intensity, which is 7 ns in advance of the main pulse is employed. Here, a clean main pulse with a minimum amount of ASE (Amplified spontaneous emission) is essential. Experimentally, the intensity ratio of the prepulse is optimized by tuning the delay time of the Pockel cell in the laser system in the range between 10^{-3} and 10^{-5}, while the consequent preplasma density and scale are varied and simultaneously monitored, as introduced in Fig. 1. Accordingly, the preplasma scale can be obtained experimentally by measuring the distance of the X-ray source position coordinates between the case without prepulse and with prepulse at various intensity ratios.[28] In the optimal case for the collimated TSE observation where the intensity ratio is about 2.5×10^{-4}, the preplasma scale is measured to be about 100 μm. Correspondingly, the wavelength shift of the incident laser from the incident spectrum to the scattered spectrum of the SBRS is measured to be around 220 nm, as shown in Fig. 2. Hence, the optimal preplasma density during the interactions is $n_e = \omega_{epw}^2 m\varepsilon_0/e^2 = (\omega_s - \omega_0)^2 m\varepsilon_0/e^2 = 1.0 \times 10^{20}/\text{cm}^3$, which is approximately $0.1N_c$, where N_c is the critical density of plasma.

Then, we start with the investigation of the highly collimated and reproducible TSE beams generation by variously optimizing the experimental parameters. We altered specifically the laser prepulse condition, especially the prepulse intensity ratio, to optimize the TSE beam quality. As mentioned above, at the optimized ratio between prepulse and main pulse intensities of around 2.5×10^{-4} for producing low-divergence TSE beam, underdense preplasma with a plasma density of about $0.1N_c$ and a preplasma scale of about 100 μm is created. From the six successive example images in Fig. 3 with equivalent experimental condition (considering the laser intensity jitter in the range of $\pm 6\%$), we observed well concentrated and intense electron jets, which are propagating along the target surface. These electron beams are reproducibly generated with low divergence and good beam pointing-stability. Since the detector is set around 15 cm away from the laser focus spot on the target, the beam size (FWHM) on the detector is measured to be at minimum 3 mm. Consequently, the divergence of the obtained TSE jets was calculated to be

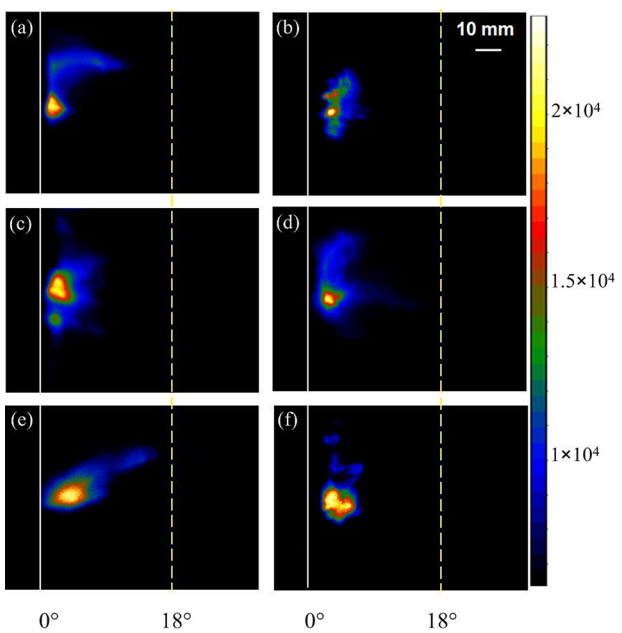

FIG. 3. The TSE beam images detected by EMCCD, which show the spatial angular distribution of the TSE beam at the optimized ratio between prepulse and main pulse intensities of around 2.5×10^{-4} and laser incident angle of 72°. The solid (white) line represents the target-surface direction at 0° and the dashed (yellow) line represents the laser specular direction at 18°. The color bar shows the relative intensity of the TSE signals on the phosphor plate.

20 mrad. Compared to recently published experimental results,[17] we reduced the divergence angle by half while keeping the pointing stability to less than $\pm 1^\circ$.

On the basis of the stable output of the TSE beams, we studied the corresponding electron energy spectrum, as seen in the inset of Fig. 4, which is detected by a well-calibrated ES. Obviously, a monoenergetic electron bunch is generated and by analyzing the electron signals on the IP stripe, a main, narrow-band peak at 0.55 MeV is shown in Fig. 4. The peak indicates that MeV monoenergetic TSE beams are obtained with a small energy spread of $\Delta E = \delta E/E = 0.028\text{MeV}/0.550\text{MeV} = 5.0\%$. We calculate the total charge of the whole electron beam by integrating the electron number as a function of electron energy in the frame of the energy spectrum and the result is up to 30 pC per laser shot. Compared to the previous results,[17–20] the energy spread is reduced by more than a factor of six while maintaining a sufficient total charge. Therefore, we are able to demonstrate that large scale near-critical density plasma environment is required for producing the optimized-quality monoenergetic TSE beam with low divergence. This result also provides a good guidance to the following numerical simulations.

In order to clarify the physical mechanism of our observed monoenergetic TSE bunches, generated with a small divergence, a numerical simulation was performed by using a 2D3V OOPIC code.[29] According to our experimental condition, we used a 70 fs, *p*-polarized Gaussian laser pulse with a 3.5 μm waist, incident at $\theta = 72^\circ$ on a two-layer plasma, composed of a 9.5λ thick plasma slab with a uniform density of 0.25*Nc* on top of a plasma wall with a critical density, where λ and *Nc* denote the laser wavelength and critical density, respectively. Here, we assume that the plasma is uniform and underdense after a 7 ns expansion in an ion-acoustic velocity. Laser pulses are partially reflected at a certain plasma density (the turning point), given by $N = \gamma \times \cos^2\theta \times N_c$. Taking into account the relativistic Lorenz factor $\gamma = (1 + \alpha_0^2/2)^{1/2} \approx 2.3$, the turning point is at 0.23*Nc* for an incident angle of 72°. The applied laser intensity is given by the normalized vector potential $\alpha_0 = eE/m\omega c \approx 3.0$, considering the maximum electric field amplitude of the laser of 1.34×10^{13} V/m. Considering the density steepen effect, the grazing incident laser pulses reflect before reaching the critical density wall due to the strong ponderomotive force. Hence, the penetration depth is less than 4 μm. Figure 5(b) shows a snapshot of the electric field distribution near the target surface during the laser-plasma interactions. While in the turning point most of the laser pulses are reflected by the plasma slab, as seen in Fig. 5(b), only a part of the laser pulses remains in the plasma and continues propagating along the target surface due to the strong modulation by the self-generated electromagnetic field near the edge of the plasma. The peak electric field amplitude of the remaining pulses reaches 1.36×10^{13} V/m, which is even higher than the incident pulses, with the field potential $\alpha_0 = eE/m\omega c \approx 3.4$, where ω denotes the laser frequency. The duration of the remaining pulses is estimated to be only about 10 fs. Thus, the ultra-short ultra-intense pulses push the plasma electrons away and a bubble like structure is formed, as shown in Fig. 5(a), similar to the wake field acceleration[30] in laser-gas interactions. Fig. 5(a) also shows clearly that several periods of plasma wave structures exist after the bubble, which are typical for the traditional wake field acceleration phenomena. The transverse radius of the "bubble" is approximately equal to one order of plasma wavelength $\lambda_p = 1.6\,\mu$m. Then, the bubble structure travels for about 20 μm before it collapses. As seen in Figs. 5(c) and 5(d), the transverse electric field to the target surface $E_\perp$ is calculated to be 2 TV/m

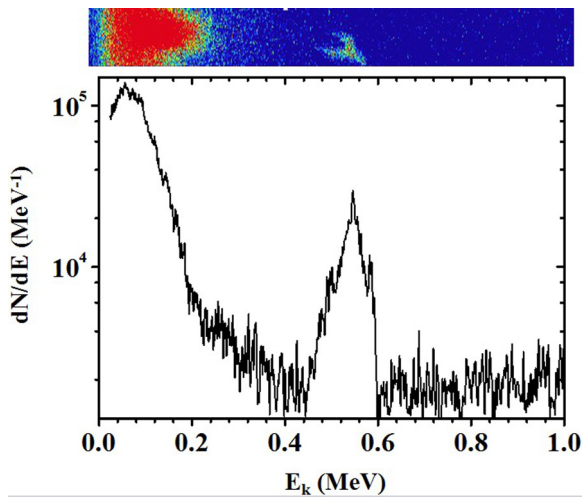

FIG. 4. Typical energy spectrum of the TSE beam. The inset represents the TSE signals on the IP inside the ES.

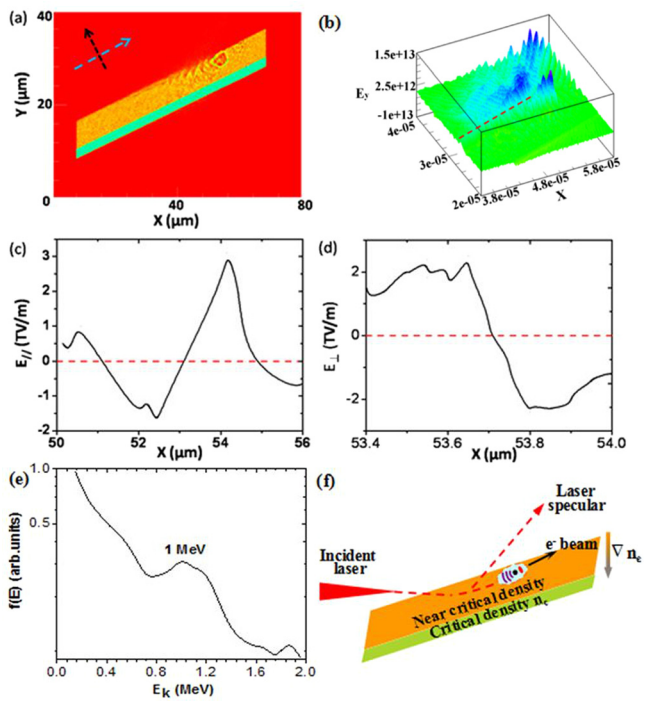

FIG. 5. 2D PIC simulation results. (a) Plasma density distribution near the target surface, where the dashed (blue) arrow represents longitudinal electric field direction, and the dashed (black) arrow represents transverse electric field direction. (b) Electric field distribution near the target surface, the dashed (red) line represents the target surface. (c) Intensity of the longitudinal electric field in bubble, and the dashed (red) line shows the electric field where $E = 0$. (d) Intensity of the transverse electric field in bubble. (e) Energy spectrum of the electrons inside the bubble. (f) Theoretical model for the wake field acceleration mechanism in the near-critical-density plasma.

which is high enough to confine the electrons in a very small divergence, while the longitude electric field $E_{//}$ is to be 1.5 TV/m, which is one order of magnitude more intense than the wake field in gas plasma.[31] Thus, during this short period, the strong electromagnetic fields in the "bubble" trap the remaining bunch of electrons and accelerate them until the bubble collapses. This special distribution of the electric fields in the bubble structure could generate the monoenergetic electron beam effectively with a small divergence angle. The electron pulse duration is estimated to be about 15 fs judging from the longitudinal spatial size of the beam in Fig. 5(a). The corresponding simulated energy spectrum, shown in Fig. 5(e), exhibits a single peak at around 1.0 MeV, qualitatively consistent with the experimental results. Analogous to the wake field theory,[31] we propose an intuitive cartoon to elaborate the TSE acceleration process, shown in Fig. 5(f). When relativistic laser pulses are incident at large angle to a large scale near critical density plasma, the ponderomotive force expels the electrons and creates a moving bubble with strong electric fields inside. Electrons with a certain energy are injected into the bubble and accelerated by the longitudinal electric field continuously. This process results in monoenergetic electron beams emission along the target surface with a small divergence angle.

As an injector in traditional accelerators, the quality of an electron beam is tightly related to the subsequent propagation of the bunch along the beam line, which is described by the normalized beam emittance. By using a typical extraction method,[32] the normalized emittance of our observed electron beams is estimated by an equation $\varepsilon = \gamma \times \pi \times \sigma_x \sigma_\theta$, where the σ_x is the rms beam size and σ_θ is estimated by the beam divergence angle. Here, the rms beam size is estimated as $\sigma_x = w_0/8$ with the laser waist w_0 experimentally. As we discussed above, the divergence angle of the TSE beam is measured to be 20 mrad, hence the normalized emittance is deduced to be 0.03 π mm mrad. We achieved an electron beam from solid target with a lower normalized emittance while maintained a high total charge (30 pC), compared to the previous results[32–35] from gas. Considering the sufficiently high electron energy of the TSE beam, loss of the charges by the Coulomb repulsion during bunch propagation procedure could be ignored. Therefore, our TSE bunch is applicable for the next generation of optimized-quality injectors in traditional accelerators.

The highly collimated and monoenergetic TSE beam could also been applied in the ICF field. In the fast ignition concept, the key point is to deliver the ignition energy sufficiently to the fuel without unnecessary energy loss. Therefore, the energy gain in the process of the ignition needs to be optimized, including the energy conversion from the laser pulses to the fast electrons, electron transmission efficiency in the target, and energy deposition to the fuel core. Because of the tight collimation, high charge, and small energy spread, the TSE beam generated by using a cone-target is of great benefit for improving the efficiency in all three steps in the fast ignition concept. According to the previous simulation[10] on the required ignition energy, if one can produce the collimated electrons in the kinetic energy range from 0.5 to 1 MeV of the preimploded shell and consequently 10^{11} neutrons, many orders of magnitude would be expected.

In summary, we demonstrate a acceleration mechanism for generating optimized-quality monoenergetic TSE beams with an extremely low normalized emittance of 0.03π mm mrad and large charge of 30 pC via a Cu bulk target irradiated by a few TW fs laser. The corresponding energy spectrum exhibited a single-energy peak at 0.55 MeV. The preplasma manipulation played a crucial role in stimulating the wake-field structure. 2D PIC simulation indicated that a bunch of electrons inside the bubble-like structure are accelerated by the wake field in a plasma with near-critical density. The time duration of the TSE beam was estimated to be 15 fs. Such a low normalized emittance, ultrashort duration, and MeV class monoenergetic electron beams could meet the requirements for applications in accelerators. In addition, this method can contribute to greatly improve the energy concentration at the ignition core by using a cone target to focus these highly collimated and monoenergetic beams in the fast ignition concept.

We thank L. T. Hudson and C. Schneider for fruitful discussions. This work was supported by the NSFC Grant No. 11334013, National key Scientific Instrument and Equipment Development Project No. 2012YQ120047, the National Basic Research Program of China (Grant No. 2013CBA01501) and the Key Research programme of CAS (KGZD-EW-T05). J.Y.M. gratefully acknowledges the financial support from the Carl-Zeiss Foundation.

[1]S. Bastiani, A. Rousse, J. P. Geindre, P. Audebert, C. Quoix, G. Hamoniaux, A. Antonetti, and J.-C. Gauthier, Phys. Rev. E **56**, 7179 (1997).
[2]M. H. Key, M. D. Cable, T. E. Cowan, K. G. Estabrook, B. A. Hammel, S. P. Hatchett, E. A. Henry, D. E. Hinkel, J. D. Kilkenny, J. A. Koch *et al.*, Phys. Plasmas **5**, 1966 (1998).
[3]Y. Sentoku, H. Ruhl, K. Mima, R. Kodama, K. A. Tanaka, and Y. Kishimoto, Phys. Plasmas **6**, 2855 (1999).
[4]T. E. Cowan, M. Roth, J. Johnson, C. Brown, M. Christl, W. Fountain, S. Hatchett, E. A. Henry, A. W. Hunt, M. H. Key *et al.*, Nucl. Instrum. Methods Phys. Res., Sect. A **455**, 130 (2000).
[5]M. I. K. Santala, M. Zepf, I. Watts, F. N. Beg, E. Clark, M. Tatarakis, K. Krushelnick, A. E. Dangor, T. McCanny, I. Spencer *et al.*, Phys. Rev. Lett. **84**, 1459 (2000).
[6]L. M. Chen, J. Zhang, Y. T. Li, H. Teng, T. J. Liang, Z. M. Sheng, Q. L. Dong, L. Z. Zhao, Z. Y. Wei, and X. W. Tang, Phys. Rev. Lett. **87**, 225001 (2001).
[7]Z. M. Sheng, Y. Sentoku, K. Mima, J. Zhang, W. Yu, and J. Meyer-ter-Vehn, Phys. Rev. Lett. **85**, 5340 (2000).
[8]H. Ruhl, Y. Sentoku, K. Mima, K. A. Tanaka, and R. Kodama, Phys. Rev. Lett. **82**, 743 (1999).
[9]R. Kodama, K. A. Tanaka, Y. Sentoku, T. Matsushita, K. Takahashi, H. Fujita, Y. Kitagawa, Y. Kato, T. Yamanaka, and K. Mima, Phys. Rev. Lett. **84**, 674 (2000).
[10]M. Tabak, J. Hammer, M. E. Glinsky, W. L. Kruer, S. C. Wilks, J. Woodworth, E. M. Campbell, M. D. Perry, and R. J. Mason, Phys. Plasmas **1**, 1626 (1994).
[11]O. A. Hurricane, D. A. Callahan, D. T. Casey, P. M. Celliers, C. Cerjan, E. L. Dewald, T. R. Dittrich, T. Döppner, D. E. Hinkel, L. F. Berzak Hopkins *et al.*, Nature **506**, 343 (2014).
[12]Y. T. Li, X. H. Yuan, M. H. Xu, Z. Y. Zheng, Z. M. Sheng, M. Chen, Y. Y. Ma, W. X. Liang, Q. Z. Yu, Y. Zhang *et al.*, Phys. Rev. Lett. **96**, 165003 (2006).
[13]Z. Li, H. Daido, A. Fukumi, A. Sagisaka, K. Ogura, M. Nishiuchi, S. Orimo, Z. Hazashi, M. Mori, M. Kado *et al.*, Phys. Plasmas **13**, 043104 (2006).

[14]H. Habara, K. Adumi, T. Yabuuchi, T. Nakamura, Z. L. Chen, M. Kashihara, R. Kodama, K. Kondo, G. R. Kumar, L. A. Lei *et al.*, Phys. Rev. Lett. **97**, 095004 (2006).
[15]L. M. Chen, M. Kando, M. H. Xu, Y. T. Li, J. Koga, M. Chen, H. Xu, X. H. Yuan, Q. L. Dong, Z. M. Sheng *et al.*, Phys. Rev. Lett. **100**, 045004 (2008).
[16]A. G. Mordovanakis, J. Easter, N. Naumova, K. Popov, P. Masson-Laborde, B. X. Hou, I. Sokolov, G. Mourou, I. V. Glazyrin, W. Rozmus *et al.*, Phys. Rev. Lett. **103**, 235001 (2009).
[17]T. Ye, J. S. Liu, W. T. Wang, C. Wang, A. H. Deng, C. Q. Xia, W. T. Li, L. H. Cao, H. Y. Lu, H. Zhang *et al.*, Phys. Rev. Lett. **109**, 115002 (2012).
[18]R. Kodama, P. A. Norreys, K. Mima, A. E. Dangor, R. G. Evans, H. Fujita, Y. Kitagawa, K. Krushelnick, T. Mizakoshi, N. Miyanaga *et al.*, Nature (London) **412**, 798 (2001).
[19]R. Kodama, H. Shiraga, K. Shigemori, Y. Toyama, S. Fujioka, H. Azechi, H. Fujita, H. Habara, T. Hall, Y. Izawa *et al.*, Nature (London) **418**, 933 (2002).
[20]J. Y. Mao, L. M. Chen, X. L. Ge, L. Zhang, W. C. Yan, D. Z. Li, G. Q. Liao, J. L. Ma, K. Huang, Y. T. Li *et al.*, Phys. Rev. E **85**, 025401(R) (2012).
[21]M. Chen, Z. M. Sheng, J. Zheng, Y. Y. Ma, M. Bari, Y. T. Li, and J. Zhang, Opt. Express **14**, 3093 (2006).
[22]T. Nakamura, S. Kato, H. Nagatomo, and K. Mima, Phys. Rev. Lett. **93**, 265002 (2004).
[23]L. Willingale, A. G. R. Thomas, P. M. Nilson, H. Chen, J. Cobble, R. S. Craxton, A. Maksimchuk, P. A. Norreys, T. C. Sangster, R. H. H. Scott *et al.*, New J. Phys. **15**, 025023 (2013).
[24]T. Tajima and S. Ushioda, Phys. Rev. B **18**, 1892 (1978).
[25]K. A. Tanaka, T. Yabuuchi, T. Sato, R. Kodama, Y. Kitagawa, T. Takahashi, T. Ikeda, Y. Honda, and S. Okuda, Rev. Sci. Instrum. **76**, 013507 (2005).
[26]C. B. Darrow, C. Coverdate, M. D. Perry, W. B. Mori, C. Clayton, K. Marsh, and C. Joshi, Phys. Rev. Lett. **69**, 442 (1992).
[27]C. Rousseaux, G. Malka, J. L. Miquel, F. Amiranoff, S. D. Baton, and P. Mounaix, Phys. Rev. Lett. **74**, 4655 (1995).
[28]L. M. Chen, P. Forget, S. Fourmaux, J. C. Kieffer, A. Krol, C. C. Chamberlain, B. X. Hou, J. Nees, and G. Mourou, Phys. Plasmas **11**, 4439 (2004).
[29]J. P. Verboncoeur, A. B. Langdon, and N. T. Gladd, Comput. Phys. Commun. **87**, 199 (1995).
[30]W. Lu, M. Tzoufras, C. Joshi, F. S. Tsung, W. B. Mori, J. Vieira, R. A. Fonseca, and L. O. Silva, Phys. Rev. Spec. Top.-Accel. Beams **10**, 061301 (2007).
[31]T. Tajima and J. M. Dawson, Phys. Rev. Lett. **43**, 267 (1979).
[32]E. Brunetti, R. P. Shanks, G. G. Manahan, M. R. Islam, B. Ersfeld, M. P. Anania, S. Cipiccia, R. C. Issac, G. Raj, G. Vieux *et al.*, Phys. Rev. Lett. **105**, 215007 (2010).
[33]G. R. Plateau, C. G. R. Geddes, D. B. Thorn, M. Chen, C. Benedetti, E. Esarey, A. J. Gonsalves, N. H. Matlis, K. Nakamura, C. B. Schroeder *et al.*, Phys. Rev. Lett. **109**, 064802 (2012).
[34]C. G. R. Geddes, Cs. Toth, J. van Tilborg, E. Esarey, C. B. Schroeder, D. Bruhwiler, C. Nieter, J. Cary, and W. P. Leemans, Nature (London) **431**, 538 (2004).
[35]N. A. M. Hafz, T. M. Jeong, I. W. Choi, S. K. Lee, K. H. Pae, V. V. Kulagin, J. H. Sung, T. J. Yu, K. H. Hong, T. Hosokai *et al.*, Nat. Photonics **2**, 571 (2008).